academicJournals

Vol. 11(7), pp. 85-95, 16 April, 2016
DOI: 10.5897/IJPS2015.4445
Article Number: C47BBD058001
ISSN 1992 - 1950

http://www.academicjournals.org/IJPS

International Journal of Physical Sciences

Full Length Research Paper

Analysis of $\pi^{\pm}-^{16}O$ elastic scattering data below, atop and above the delta resonance using inverse scattering theory

Reham M. El-Shawaf and Zuhair F. Shehadeh*

Physics Department, Taif University, Taif, Zip Code 21974, Taif, Saudi Arabia.

Received 3 December, 2015; Accepted 22 March, 2016

The simple local optical potential adopted in analyzing successfully $\pi^{\pm}-^{12}C$ elastic scattering data in the delta resonance region has been emphasized here. This is based on obtaining the same nature for the potential by extracting potential points from available $\pi^{\pm}-^{16}O$ phase shifts at 114, 163, 240 and 340 MeV using inverse scattering theory within the framework of Klein-Gordon equation. Luckily, and as expected, the obtained analytical potential form has also been used successfully in accounting for the experimental angular distributions at another nearby four energies, namely 170, 220, 230, and 270 MeV. At energies considered herein, the calculated reaction cross sections are in good agreement with available experimental ones, and are in spectral match with $\pi^{\pm}-^{12}C$ experimental ones. The nature of the real part of the potential showed a change from attractive to repulsive at about 200 MeV, and the imaginary part is dominated by the surface absorption term. In treating the pion-nucleus scattering problem, we found that there is no privacy for a doubly closed-shell self-conjugate target nucleus compared to another nucleus, at least $Z = N$ light bound nucleus, and for incident pion energies in the domain of the delta resonance region. Instead, it seems that the description of the scattering process is mainly attributed to the geometrical structure of the target nucleus. This is a first time corollary, and more investigations are needed.

Key words: Pion-nucleus potential, elastic scattering, inverse scattering theory, high energy physics.

INTRODUCTION

The pion plays an important role in nuclear physics due to its unique physical properties (Stroot, 1973) as 1) it is a generator (carrier) of the nuclear force 2) it is an important part in the nuclear many-body problem 3) it has a zero spin 4) it has a one isospin triplet 5) it has negative and positive charges that allow for neutron and proton characterization, and uncover Coulomb effects. Exceptionally, pion facilities have been established and developed to produce and accelerate these pions (Lee and Redwine, 2002). In the literature (Shehadeh, 2008),

*Corresponding author. E-mail: zfs07@hotmail.com.

PACS No: 24.10.Ht, 25.80.Dj, 11.80 m.

pions are categorized into three well-known energy regions according to their incident kinetic energies, T_π. These energy regions are the low energy region $(0 < T_\pi \le 100 MeV)$, resonance energy region $(100 < T_\pi \le 400 MeV)$ and the high energy region $(T_\pi > 400 MeV)$. In each energy region, the pion has its own mean free path, λ, which is smaller, on the order of or larger than the inter-nucleon distance, d, in the nucleus. This is an indicator whether the pion can penetrate into the nucleus or be absorbed at the nuclear surface.

In the resonance energy region, also known as the (3/2, 3/2) resonance energy which is abbreviated as (3,3) resonance energy or the delta resonance (Δ-resonance) region, $\lambda << d$ which prevents the pion from penetrating into the nucleus and only faces a complete absorption at the nuclear surface.

As the number of pion-nucleon scatterings is limited by λ, different theories, theoretical models and theoretical approaches have been proposed (Kisslinger, 1955; Fäldt, 1972; Eriscson and Weise, 1988) to describe successfully the available pion-nucleus data, mainly the angular distributions, at all angles and energies covering all energy regions. In the low energy region, several previous pion-nucleus potentials have been proposed and used to explain the available wealth of pion-nucleus scatterings data as explained in Shehadeh (2013a) and references therein. Unfortunately the success was either marginal or incomplete. This formed a strong motivation for us to search for new pion-nucleus potentials that serve well in providing a better explanation for measured angular distributions. Indeed the low energy $\pi^{\pm} - {}^{12}C, {}^{16}O, {}^{40}Ca$ elastic scattering data have been nicely explained by our potentials (Shehadeh, 2013a, 2014c; Shehadeh and Al-Shawaf, 2015) which are obtained from available phase shifts using inverse scattering theory and adopting the full Klein-Gordon equation.

In the Δ-resonance region, also several theories, theoretical models and approximations as, but not restricted to, the multiple scattering theory (Eisenberg and Koltun, 1980) including both Watson's multiple scattering theory and Glauber's multiple scattering theory (Shalaby et al., 2007), the Δ-hole formalism (Hirata et al., 1979; Kisslinger and Wang, 1976), eikonal approximation with the interacting boson model (Zhang, 1993), strong absorption model (Begum et al., 2003; Rahman and Sen Gupta, 1991), the single folding α-cluster model (El-AzabFarid and Ebrahim 2015), equivalent local Kisslinger optical potential with analytical distorted wave approximation (Safari, 2005), a density dependent optical pion-nuclear potential (Gmitro et al., 1987), local and equivalent local optical potentials (Satchler, 1992; Johnson and Satchler, 1996; Khallaf and Ebrahim, 2000; Ebrahim and Khallaf, 2005; Khallaf and Ebrahim, 2005; Akhter et al., 2001; Hong and Kim, 1999) have been used with varying degrees of success. The deficiencies of these theories are alluded to 1) fail in reproducing backward elastic scattering data for both pion charges 2) difficulty in calculation due to non-localities 3) true quantitative description of the scattering process 4) disagreement between theory and experiment especially around maximum and minimum 5) unphysical meaning for some used parameters and 6) uncertainties in the data.

It is of special importance to point out that among all proposed pion-nucleus potentials, Satchler's potential (Satchler, 1992) deserves special remembrance and commemoration. He introduced a simple local phenomenological optical potential of Woods-Saxon shape, for both real and imaginary parts, to describe the scattering data of charged pions from few nuclei in the (3,3) resonance region. Satchler's treatment was based, and for the first time, on reducing Klein-Gordon equation into a relativistic Schrödinger equation by performing some redefined kinematical quantities. Although he neglected the squared potential term, $V^2(r)/2E$, in his treatment and, in essence, has used the truncated Klein-Gordon equation and not the complete one, he achieved better results than any other study done before. As such, he recorded a distinguished great success with a witnessed novelty in his treatment. Accordingly, Satchler's treatment forms a strong inducement for analyzing several $\pi^{\pm}$ − nucleus data over the last two decades.

Recently, and in analyzing pion-^{40}Ca elastic scattering data at 163.3 MeV, Shehadeh et al. (2003), have noticed that when Satchler's potential is implemented in the complete Klein-Gordon equation, that is, considering $V^2(r)/2E$ term, the fit is no more good especially at backward angles. This was a suitable reasoning to search for an alternative potential which could successfully explain the experimental backward-angle elastic scattering angular distributions, as well as forward-angle ones, for several pion-nucleus systems. Shehadeh (1995) has obtained the nature of pion-^{40}Ca optical potential from the available phase shifts using inverse scattering theory within the framework of the complete Klein-Gordon equation. The analytical form of this potential has also been adopted in several subsequent studies (Shehadeh et al., 2011; Shehadeh, 2013b, 2014a, b), and has showed a remarkable success in accounting for all analysed pion-nucleus elastic scattering angular distributions data. As such, the same analytical form is adopted here in analyzing $\pi^{\pm} - {}^{16}O$ elastic scattering angular distributions data at eight energies ranging from 114 to 340 MeV.

THEORY

Nature of pion $-{}^{16}O$ potential

The extracted potential points, obtained from available phase shifts using inverse scattering theory within the framework of the

complete Klein-Gordon equation, have obligated the shape of the nuclear pion $-^{16}O$ potential as outlined in inverse scattering method. The obtained potential is the same as the one used in the pion $-^{12}C$ case (Shehadeh, 2014a), and has the following analytical form:

$$V_N(r)=\frac{V_o}{1+\exp\left(\frac{r-R_o}{a_o}\right)}+\frac{V_1}{\left[1+\exp\left(\frac{r-R_1}{a_1}\right)\right]^2}+i\frac{W_2}{1+\exp\left(\frac{r-R_2}{a_2}\right)}+i\frac{W_3\exp\left(\frac{r-R_3}{a_3}\right)}{\left[1+\exp\left(\frac{r-R_3}{a_3}\right)\right]^2} \quad (1)$$

It is clear that $V_N(r)$ consists of four potential terms as the sum of two real and two imaginary terms. The two real terms are of Woods-Saxon and squared Woods-Saxon forms, while the imaginary ones are of Woods-Saxon and surface Woods-Saxon forms. This analytical nuclear potential, which is Satchler's potential (Satchler, 1992) consummated by the squared Woods-Saxon real term, has been used before in analysing successfully pion-nucleus elastic scattering angular distributions data over all angular ranges and wide range of energies (Shehadeh, 1995, 2013b, 2014a, b; Shehadeh et al., 2011). The Coulomb potential, $V_C(r)$, is substituted for by a constant of ± 4.2 MeV for $\pi^{\mp}$, respectively, according to Stricker's prescription(Stricker, 1979):

$$V_c=\pm\frac{Z_T e^2}{R_c} \quad (2)$$

Where $Z_T=8$, $e^2=1.44$ MeV.fm and $R_c=2.74$ fm are the atomic number of the target nucleus, the square of the electronic charge in nuclear units and Coulomb radius, respectively.

As usual, the potential in (1) is inserted in the radial part of Klein-Gordon equation given by:

$$\left[d^2/dr^2+k^2-U(r)-\frac{\ell(\ell+1)}{r^2}\right]R_{n\ell}(r)=0 \quad (3)$$

with

$$k^2=\left(E^2-m^2c^4\right)/\hbar^2c^2 \quad (4)$$

$$U(r)=\frac{2E}{\hbar^2c^2}\left[V(r)-V^2(r)/2E\right] \quad (5)$$

where $R_{n\ell}(r)$ is the r times the radial part of the wave function for a spherical symmetric external potential. In Equations (4) and (5), E, m, c and $V(r)$ are the actual pion energy, effective pion mass, velocity of electro-magnetic wave in vacuum and complex pion-nucleus potential, $V(r)=V_N(r)+V_C(r)$, respectively. The actual pion energy and its effective mass are calculated following Satchler's assertion (Satchler, 1992), and will not be repeated here. To calculate the differential and reaction cross sections, $d\sigma/d\Omega$ and σ_r, respectively, defined as :

$$\frac{d\sigma}{d\Omega}=\left|f_c(\theta)+\frac{1}{2ik}\sum_{\ell=0}^{\infty}(2\ell+1)\exp(2i\sigma_\ell)\left[\exp(2i\delta_\ell)-1\right]P_\ell(\cos\theta)\right|^2 \quad (6)$$

$$\sigma_r=\frac{\pi}{k^2}\sum_{\ell=0}^{\infty}(2\ell+1)\left[1-|S_\ell|^2\right] \quad (7)$$

one needs to know the complex nuclear phase shifts δ_ℓ. In Equations (6) and (7), $f_c(\theta)$ is the point Coulomb scattering amplitude, σ_ℓ is the point Coulomb phase shift, $P_\ell(\cos\theta)$ is the Legendre polynomial, and $S_\ell=e^{2i\delta_\ell}$ is the S-matrix.

For each partial wave ℓ, the phase shift δ_ℓ is calculated by matching the logarithmic derivatives of the inner and outer solutions at the cutoff radius $r=R$ where the nuclear potential is turned off. The inner solution, for $r<R$, is obtained by solving (3) numerically and having the wave function $\psi_\ell(r)$ satisfies the boundary condition,

$$\lim_{r\to 0}\psi_\ell(r)\approx(kr)^{\ell+1} \quad (8)$$

The outer solution, for $r\geq R$, is the well-known one expressed as:

$$\psi_\ell(r)=F_\ell(\gamma,kr)+\frac{\exp(2i\delta_\ell)-1}{2i}\left[G_\ell(\gamma,kr)+iF_\ell(\gamma,kr)\right] \quad (9)$$

where F_ℓ and G_ℓ are the relativistic regular and irregular Coulomb wave functions (Shehadeh, 2015a).

Inverse scattering method

Although the inverse scattering theory has been explained well in our previous work (Shehadeh, 2009), it will be summarized here for its fundamentality and as being a backbone in this investigation. The method relies on transforming the second order differential equation given in Equation (3) and also expressed as:

$$\left[\frac{d^2}{dr^2}+\frac{2(\ell+1)}{r}\frac{d}{dr}+k^2-U(r)\right]\varphi_{n\ell}(r)=0 \quad (10)$$

with

$$\varphi_{n\ell}(r)=(kr)^{-(\ell+1)}R_{n\ell}(r) \quad (11)$$

into a difference equation of the following form :

$$\varphi_{n+1}=A_n(\ell)B_n(\ell)\varphi_n+C_n(\ell)\varphi_{n-1} \qquad n=1,2...N \quad (12)$$

In this equation, the quantities $A_n(\ell)$, $B_n(\ell)$ and $C_n(\ell)$ are defined as:

$$A_n(\ell)=2-\Delta^2k^2+\Delta^2U_n \quad (13)$$

$$B_n(\ell)=n/(\ell+1+n) \quad (14)$$

$$C_n(\ell) = (\ell + 1 - n)/(\ell + 1 + n) \quad (15)$$

where Δ is obtained by dividing the range, R, of $U(r)$ in N equal parts so that $R = N\Delta$ and the point $r = n\Delta$ with n being an integer.

The most important of these quantities is $A_n(\ell)$ as it contains U_n which is the value of U at the n-th point and, as such, one can obtain the inverted potential points. Since the nuclear part of the potential is negligible for $r > R$, the logarithmic derivative for a given ℓ, $Z_N(\ell)$, is approximated by replacing the first derivative by central difference for $n = N$, that is, $R = N\Delta$, and has the following form:

$$Z_N(\ell) = \left(\frac{N}{2}\right)\left(\frac{\varphi_{N+1} - \varphi_{N-1}}{\varphi_N}\right) \quad (16)$$

It is clear that the function $Z_N(\ell)$ can be evaluated from (12) for $n = N$,

$$\frac{\varphi_{N+1}}{\varphi_N} = A_N(\ell)B_N(\ell) + C_N(\ell)/(\varphi_N/\varphi_{N-1}) \quad (17)$$

Where $A_N = 2 - \Delta^2 k^2$ for $U_N = 0$. So at the nuclear surface, that is, $r = R$, one gets :

$$\frac{\varphi_N}{\varphi_{N-1}} = \frac{[C_N(\ell) - 1]}{\left[\frac{2}{N}Z_N(\ell) - A_N(\ell)B_N(\ell)\right]} \quad (18)$$

The partial wave ℓ takes the values ranging from zero to the largest partial wave number plus one in integer number steps, that is, $\ell = 0, 1, 2, ..., L$ with $N = L + 1$ where L being the largest partial wave number. From Equation (15) there is always an ℓ_n that makes $C_n(\ell_{N-n}) = 0$. Considering first the point directly inside the surface, that is, for $n = N - 1$, one has:

$$A_{N-1}(\ell_1) = \frac{1}{B_{N-1}(\ell_1)}\frac{\varphi_N(\ell_1)}{\varphi_{N-1}(\ell_1)} \quad (19)$$

Continuing this inward iteration, all the points A_{N-j} for $j = 2, 3, ..., N-1$ can be calculated by using the relation:

$$A_{N-j}(\ell_j) = \frac{1}{B_{N-j}(\ell_j)}\left[\frac{C_{N+1-j}(\ell_j)}{-A_{N+1-j}(\ell_j)B_{N+1-j}(\ell_j) + ...}\frac{C_{N-2}(\ell_j)}{-A_{N-2}(\ell_j)B_{N-2}(\ell_j) + .}\frac{C_{N-1}(\ell_j)}{-A_{N-1}(\ell_j)B_{N-1}(\ell_j) + \varphi_N(\ell_j)/\varphi_{N-1}(\ell_j)}\right] \quad (20)$$

Knowing $A_n's$, Equations (13) and (5) can be used to calculate U_n and $V_n(r)$ at all n corresponding points.

RESULTS AND DISCUSSION

The inverted potential points, obtained from available phase shifts using inverse scattering theory within the framework of the full Klein-Gordon equation, were used as a guide to determine the nature of the pion $-^{16}O$ potential. These phase shifts are available only at four pion's incident kinetic energies (Fröhlich et al., 1981), namely 114, 163, 240 and 340 MeV (lab.) in the energy region under consideration. Also large angle data exist at the lowest three energies (Albanese et al., 1980). For each of these four energies the parameters of the adopted potential in Equation (1) have been changed to keep the analytical form of the potential, both real and imaginary, in a reasonably nice match with the inverted potential points and, simultaneously, to provide the possible best fit to the angular distributions. Luckily the measured elastic differential cross sections are available for the scatterings of both positive and negative pions from oxygen-16 nucleus, and the calculated differential cross sections are in good agreement with the measured ones. The potential parameters that fulfil these two constraints consist of six fixed ones: $a_0 = 0.474\,fm$, $a_1 = 0.333\,fm$, $W_2 = -30MeV$, $R_2 = 2.53\,fm$, $a_2 = 0.766\,fm$, $R_1 = 1.65\,fm$ except at the highest two energies 270 and 340 MeV where only R_1 is changed to 2.75 and 2.65 fm, respectively; and the other six parameters were subject to change as listed in Table 1. It is worthwhile to mention that the modified versions of the inverse scattering code for non-identical particles and the hard core code (Alam and Malik, 2008) were used in this investigation.

Benefitting from these potential parameters, which form the nature of the potential at each of the four energies 114, 163, 240 and 340 MeV, and their remarkable success in explaining the measured angular distributions (Albanese et al., 1980; Bason et al., 1981), the potential parameters at the other four nearby energies, namely 170, 220, 230, and 270 MeV, were also determined. In fact, the theoretical calculations obtained by these parameters, the fixed ones and changed ones indicated in Table 1, are found to be in good agreement with the available data (Bason et al., 1981; Blecher et al., 1974;

Table 1. The changed six potential parameters $V_o(in\ MeV)$, $R_o(in\ fm)$, $V_1(in\ MeV)$, $W_3(in\ MeV)$, $R_3(in\ fm)$ and $a_3(in\ fm)$ used in Equation (1) for incident charged pions on ^{16}O target at energies $T_\pi(in\ MeV)$, in lab. system, noted in column one. The average values of our calculated reaction cross sections $\overline{\sigma_r}(theor)$ in millibarns, noticed in column ten, are compared with the extracted ones $\overline{\sigma_r}$ (Walker, 1973).

T_π	***Pions***	V_o	R_o	V_1	W_3	R_3	a_3	$\sigma_r(theor)$	$\overline{\sigma_r}(theor)$	$\overline{\sigma_r}(\text{Walker,1973})$
114	π^-	-25	1.50	-130	-145.6	3.00	0.450	568.6	573.3	555
	π^+	-25	1.50	-130	-115.6	3.20	0.450	578.0		
163	π^-	-15	3.05	-130	-370.6	2.05	0.570	580.5		
	π^+	-33	3.05	-120	-370.6	2.05	0.570	600.2	590.4	585
170	π^-	-10	3.95	-140	-260.6	2.10	0.600	576.1		
	π^+							584.4	580.2	575
220.0	π^-	+45	2.50	-80	-175.6	2.60	0.420	461.1		
	π^+							465.8	463.4	485
230	π^-	+80	2.50	-25	-175.6	2.60	0.420	450.0		
	π^+							454.1	452.0	460
240	π^-	+65	2.75	+20	-130.6	2.60	0.420	416.0		
	π^+	+65	2.45	-60	-115.6	2.60	0.480	418.8	417.4	425
270	π^-	+50	2.90	+45	-115.6	2.57	0.420	381.0		
	π^+							384.2	382.6	Not Available
340	π^-	+20	3.65	+60	-115.6	2.27	0.420	362.7	364.1	Not Available
	π^+							365.5		

Koch and Sternheim, 1972) for the scattering of either negative or positive pions from ^{16}O-nucleus. All data available in laboratory system (Blecher et al., 1974; Koch and Sternheim, 1972) were converted to the centre of mass system. In general, and at all eight energies considered herein, a good agreement between data and theoretical predictions was obtained.

To hold a comparison between $\pi^- - ^{16}O$ and $\pi^- - ^{12}C$ potential parameters, one may notice that the three diffuseness parameters (a_o, a_1, a_2) have the same values in both cases. Also the ratio between R_1-values in $\pi^- - ^{16}O$ and $\pi^- - ^{12}C$ equals 1.1 which is the same ratio for R_2, and also for $A_2^{1/3}/A_1^{1/3} = (16)^{1/3}/(12)^{1/3} = 1.1$ which means that R_1 and R_2 follow the $A^{1/3}$ rule. It is worth noticing that six potential parameters, namely a_o, a_1, a_2, R_1, R_2 and W_2 were kept fixed. In addition, the behaviour of the two changed parameters V_o and V_1 is similar for both $\pi^- - ^{16}O$ and $\pi^- - ^{12}C$ cases, that is, the depth of the real Woods-Saxon term, V_o, and the height of the real squared Woods-Saxon term, V_1, change with energy in such a way that result in a total real part that turns from attractive to repulsive at about 200 MeV. So the interplay between the two real terms decides on the general shape and nature of the real part. A similar picture for the change of the real part from attractive to repulsive has also been observed in nucleon-nucleon scattering at about 200 MeV. As the energy of the incident nucleon increases, the distance between interacting nucleons decreases and a nucleon-nucleon repulsive potential arises due to color forces between quarks. With the same analogy one can say that as the incident pion's kinetic energy increases the pion-nucleon interaction distance gets smaller but to a certain distance where the color neutrality of the pion may be violated. Therefore a repulsive force kicks in and the residual force is changed to repulsive.

On the other hand the depth of the imaginary part is most pronounced at 163 MeV which is also reflected in the highest reaction cross section. This creates no wonder as the surface imaginary potential term plays a

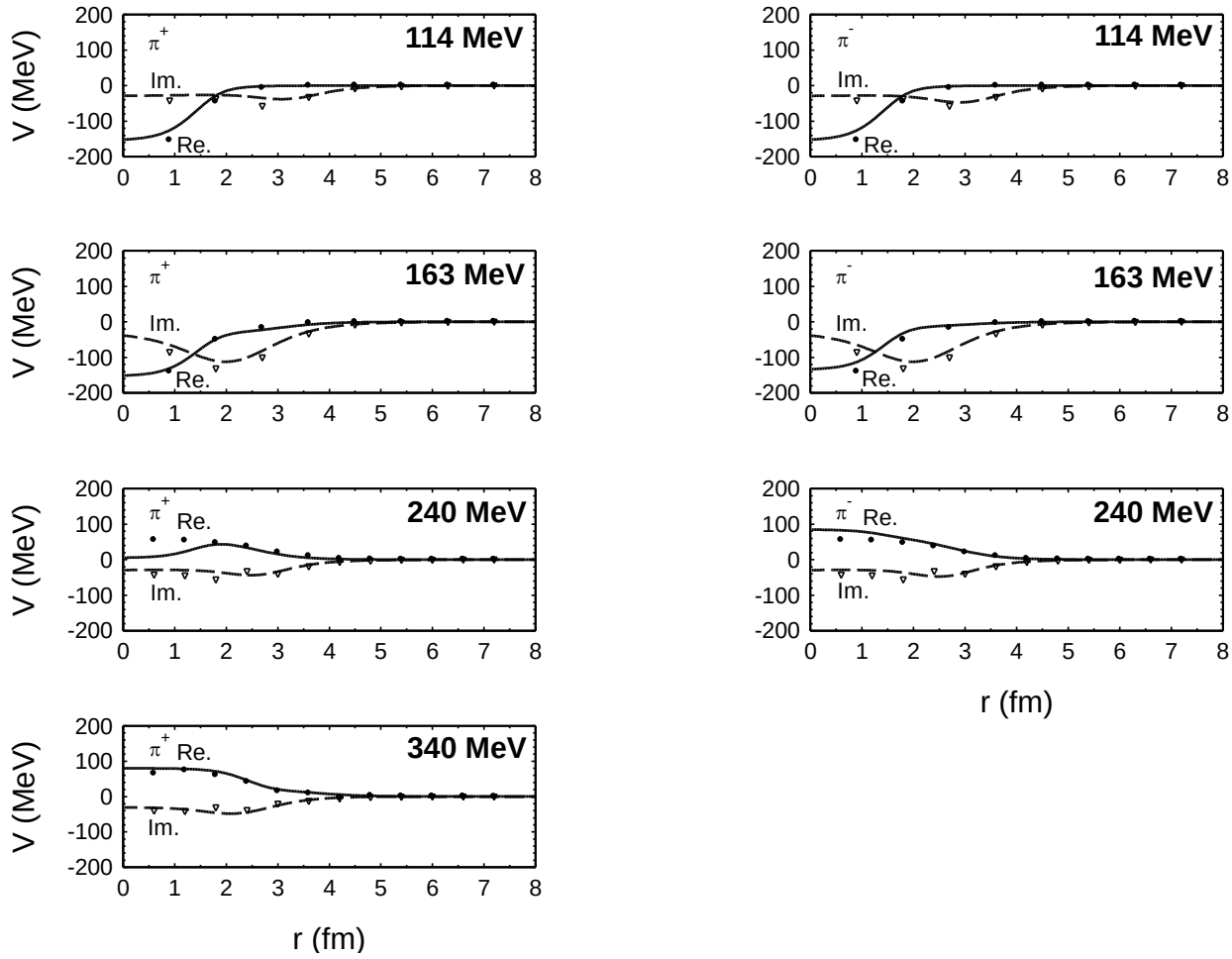

Figure 1. The analytical forms of the real (solid lines) and imaginary (dashed lines) parts of the potentials, used in analyzing elastic scattering data, are shown along with the inverted real (solid circles) and imaginary (empty triangles) potential points at 114, 163, 240 and 340 MeV incident pion kinetic energies.

dominant role in the pion's absorption at the nuclear surface for incident energies in the Δ-resonance region. Nevertheless, the contribution of the volume imaginary part in the absorption is small. With all this, one may notice the congruence between the potential parameters for both $\pi^- - {}^{16}O$ and $\pi^- - {}^{12}C$ elastic scatterings.

As pointed out, the inverse scattering theory has also been used here in predicting the pion-oxygen potentials at 114, 163, 240 and 340 MeV, where phase shift analyses are available. These four energies are vivid samples of below, atop and above resonance. The obtained inverted potential points have been used as a guide in predicting the nature of the pion-nucleus potential at each of the corresponding pion's incident kinetic energy, T_π. The parameters in Equation 1 are parameterized to keep the analytical forms, real and imaginary, of the potential very close to the inverted potential points and, simultaneously, provide the possible best fit to the measured angular distributions. The capability and success of these potentials in fitting the elastic differential and integral cross sections data (Albanese et al., 1980; Bason et al., 1981) consolidate the exceptional role played by the inverse scattering theory in investigating pion-nucleus scatterings. Such a role is also clear in determining alpha-alpha (Shehadeh, 2015b), alpha-nucleus (Alam and Malik, 1990), and nucleus-nucleus (Alam and Malik, 1991) potentials. For all energies considered herein, the calculated $\pi^\pm - {}^{16}O$ elastic differential cross sections compared to the experimental ones are shown in Figures 2 and 4. The analytical forms of the potentials, both real and imaginary parts, are displaced in Figures 1 and 3 which clearly show the attractive nature of the imaginary part and the gradual change in the real part, with T_π, from attractive to repulsive at about 200 MeV. At the four bombarding energies 114, 163, 240 and 340 MeV where phase shifts are available, Figure 1 also shows the inverted potential points drawn as solid circles and empty triangles for real

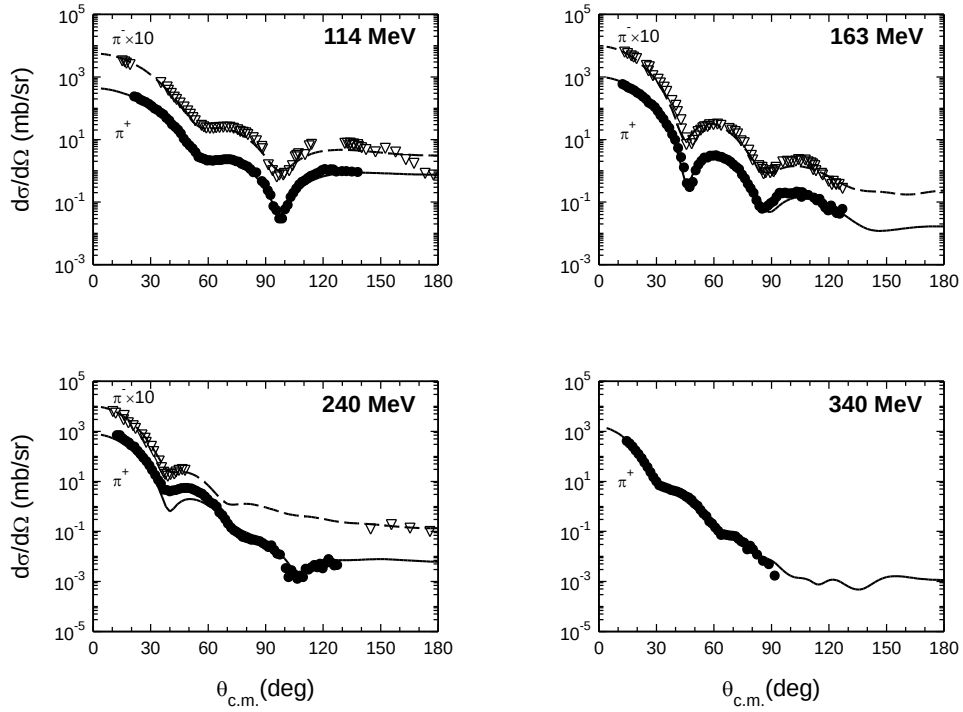

Figure 2. The calculated elastic differential cross sections, drawn as solid and dashed lines for positive and negative pions, respectively, compared to the experimental data (Albanese et al., 1980; Bason et al., 1981), represented by solid circles and empty triangles, as a function of center of mass angle $\theta_{c.m.}$.

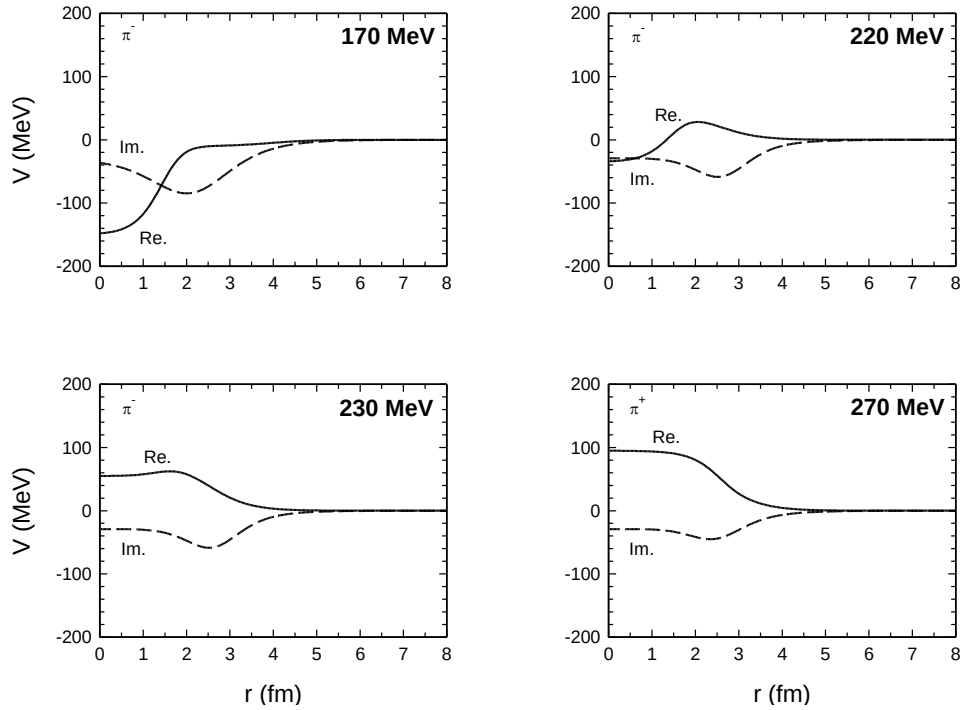

Figure 3. The analytical forms of the real (solid lines) and imaginary (dashed lines) parts of the potentials used in analyzing the $\pi^- - ^{16}O$ elastic scattering data at $T_\pi = 170$, 220 and 230 MeV, and in analyzing $\pi^+ - ^{16}O$ elastic scattering data at $T_\pi = 270$ MeV.

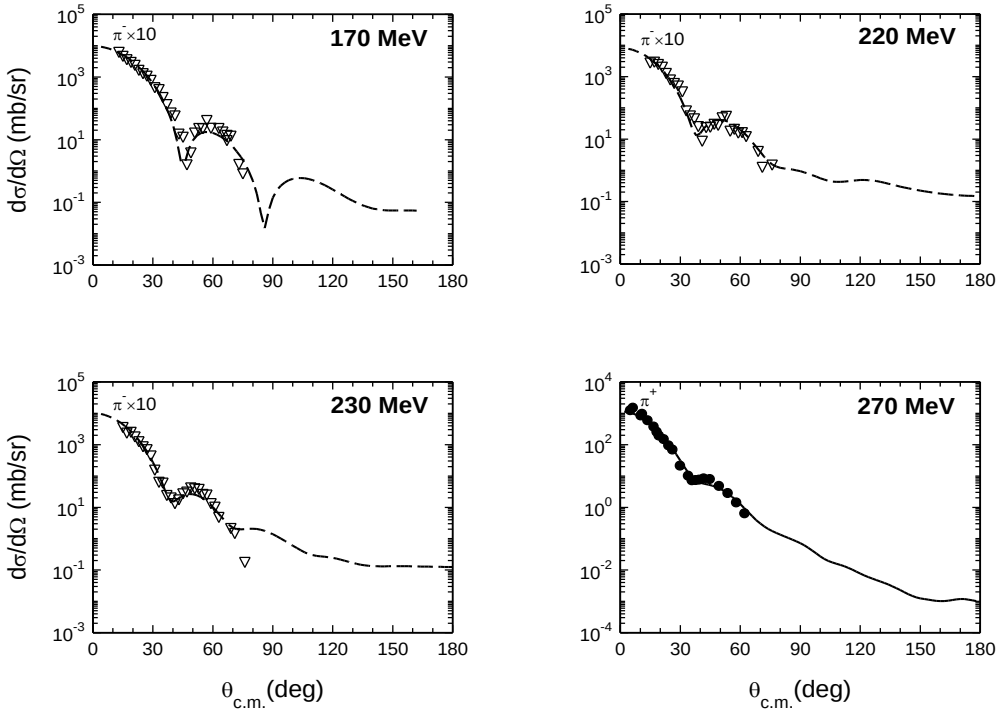

Figure 4. The calculated elastic differential cross sections (dashed lines) for negative pions and (solid line) for positive pions, are compared with the experimental values, represented by empty triangles (Blecher et al., 1974) and solid circles (Koch and Sternheim, 1972), as a function of center of mass angle $\theta_{c.m.}$.

and imaginary parts of the potential, respectively, and these points are in a good match with the analytical forms. The reasonable number of phase shifts and the proper choice of the cutoff radius (Alam, 1991) contribute positively in obtaining more reliable inverted potential points, and then correct potential parameters.

The harmony in the behaviours of the potentials, real and imaginary parts, and the calculated reaction cross sections for both $\pi^- - {}^{16}O$ and $\pi^- - {}^{12}C$ nuclear systems is very obvious. In fact our calculated reaction cross sections and W_3-values are nicely correlated as both of them represent absorption to nonelastic channels. Also it is worth to notice that the calculated reaction cross sections for $\pi^- - {}^{16}O$ are, as expected, greater than the ones for $\pi^- - {}^{12}C$ at all energies under consideration. This is clearly displaced in Figure 5. Nevertheless, our calculated reaction cross sections satisfy the $A^{2/3}$ rule in the resonance energy region (Walker, 1973), especially at the resonance-peak. This may indicate that a doubly closed-shell self-conjugate target nucleus did not differ significantly from a non-doubly and/or self-conjugate one, especially for light nuclei as oxygen-16 and carbon-12 with equal numbers of protons *Z* and neutrons *N*, i.e. *Z* = *N*, for each, in determining the gross behaviour of the scattering process. Surely this needs more investigation. In addition, one may notice that our calculated reaction cross sections are in good agreement with experimental and reported theoretical values (El-Azab Farid and Ebrahim, 2015; Albanese et al., 1980; Walker, 1973; Clough et al., 1974), with the consideration of a downward shift in the peak of the reaction cross section by about 15 MeV (Phatak et al., 1973).

It is also interesting to notice that the second minimum, in the calculated $\pi^- - {}^{16}O$ elastic differential cross sections, starts disappearing at energies between 200 and 340 MeV, faster than its counterpart for $\pi^+ - {}^{16}O$. The depth of the minima reveals important information about Coulomb effects, and may reduce the number of ambiguities in a phase shift analysis, in studying the scattering of both positive and negative pions from a nucleus (Ingram et al., 1978; Piffaretti et al., 1977; Germond and Wilkin, 1977). In addition, only two observed minima are observed as there is no complete experimental very-large backward-angle elastic differential cross sections at these energies. Very accurate large and very large angle data are also necessary in solving the uniqueness potential problem, and in solving an open long debate over the ambiguities in the potential parameters (Shehadeh, 2013b; Albanese et al., 1980). Also such an accurate data would confirm the superiority of a theoretical model in explaining pion-nucleus scattering mechanisms (Albanese et al., 1980). In fact this was also very crucial in adding the squared Woods-

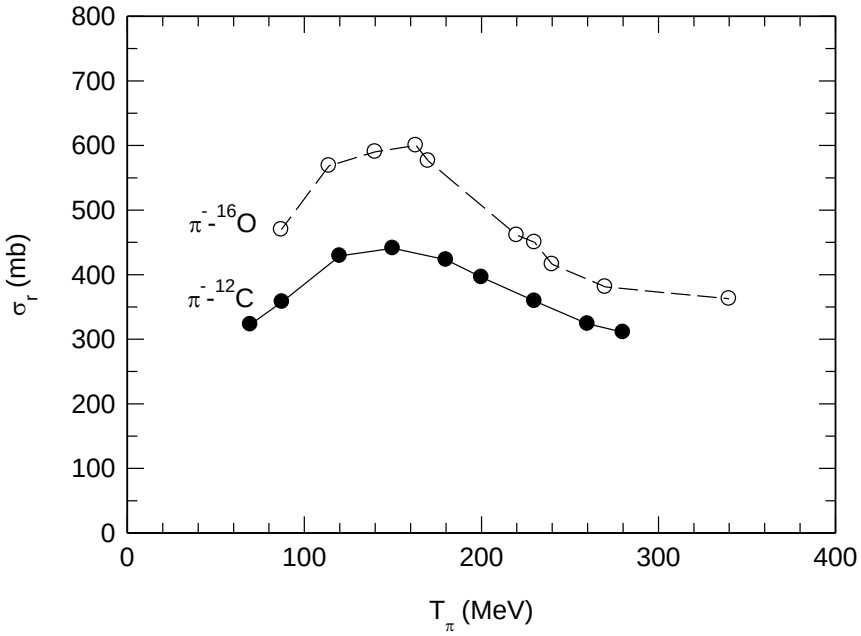

Figure 5. Our calculated $\pi^- - ^{16}O$ cross sections, represented by open circles, are compared to the experimental ones for $\pi^- - ^{12}C$, represented by solid circles (Binon et al., 1970). The values for both cases are in harmony, and are higher for $\pi^- - ^{16}O$ as expected. The solid and dashed lines are just to guide the eye.

Saxon real term to Satchler's potential to obtain a nice fit to large-angle scattering data (Shehadeh et al., 2003). As a whole, this sheds light on both nuclear and Coulomb parts of the potential.

CONCLUSIONS

This study confirms the capability of our adopted simple local optical potential in explaining well the measured $\pi^{\pm} - ^{16}O$ elastic angular distributions at eight energies below, a top and above resonance. The success of this potential is confirmed by providing a simultaneous theoretical explanation for the measured differential and integral cross sections for the scattering of both positive and negative pions from ^{16}O nucleus. It is obvious that the calculated reaction cross sections, for the scattering of charged pions from oxygen-16 nucleus, are in nice agreement with the published values. Also they cope up with their counterparts for the scattering of charged pions from carbon-12 nucleus; and they both follow the $A^{2/3}$ rule for the obtained crest values at resonance. Also the changed pattern of the real part of the potential from attractive to repulsive at about 200 MeV is emphasized. The interplay between the two real potential terms is significant in shaping the real part of the potential, and supports the addition of the squared Woods-Saxon potential term to the real part of Satchler's potential. The inverted potential points, obtained by using inverse scattering theory from available phase shifts within the framework of Klein-Gordon equation, play an exceptional role in parameterizing the potential parameters and, as such, in determining the correct pion-oxygen potentials at all energies under consideration. In addition, such parameterization reveals that both R_1 and R_2 follow the $A^{1/3}$ rule. Also, and for the first time, this investigation establishes that the target nucleus, being doubly closed-shell self-conjugate one or not, did not have any merit in the treatment of pion-nucleus scattering problem, especially for $N = Z$ tightly bound light target nuclei ^{16}O and ^{12}C, and for incident pion energies in the vicinity of the (3,3) resonance.

Conflict of Interests

The authors have not declared any conflict of interests.

ACKNOWLEDGEMENTS

The authors are very pleased to acknowledge the encouragement and financial support of the Deanship of Scientific Research at Taif University for carrying out this investigation. Our special thanks go to Prof. Moh'd Abu-Jafar for sharing his computer expertise. This paper is

dedicated to the blessed soul of Prof. F. B. Malik who suggested this important investigation.

REFERENCES

Akhter Md, Sultana S, Sen Gupta H, Petersen R (2001). Local optical model studies of pion-nucleus scattering. J. Phys. G. Nucl. Part. Phys. 27:755-771.

Alam MM (1991). PhD Thesis, Department of Physics, Southern Illinois University, Illinois, USA.

Alam MM, Malik FB (2008). Private communications, unpublished.

Alam MM, Malik FB (1990). Nature of the $\alpha-^{12}C$ Potential at Low Energy Using Inverse Scattering Method. Phys. Lett. B. 237:14-18.

Alam MM, Malik FB (1991). An Inverse Scattering Method for Identical Particles. Nucl. Phys. A. 524:88-94.

Albanese JP, Arvieux J, Bolger J, Boschitz E, Ingram CHQ, Jansen J, Zichy J (1980). Elastic Scattering of Positive Pions by ^{16}O Between 80 and 340 MeV. Nucl. Phys. A 350:301-331.

Bason E, Bos K, Bressani T, Chiavassa E, Costa S, Davies JD, Dellacasa G, Frame D, Gallio M, Jovanovich JV, Kernel G, Lourens W, Michaelis EG, Mirfakhrai N, Musso A, Panighini M,playfer SM, Rapetti M, Sever F, Stanovnik A, Tanner NW, Dantzig R, Eijk CWE, Doesburg V, Zephat AG (1981). Backward Elastic Scattering of Negative Pions from Oxygen in the (3,3) Resonance Region. CERN-EP-INT-81-04:1-13.

Begum L, Nahar W, Haque S, NasminRahman S, Rahman Md (2003). On Pion-Nucleus Scattering.The Abdussalam International Centre for Theoretical Physics, Trieste, Italy, 2003 (IC/2003/51); *ibid* (IC/2003/40). Available at : http://www.ictp.trieste.iy/~pub_off.

Binon F, Duteil P, Garron JP, Gorres J, Hugon L, Peigneux JP, Schmit C, Spighel M, Stroot JP (1970). Scattering of Negative Pions on Carbon. Nucl. Phys. B17:168-188.

Blecher M, Gotow K, Anderson DK, Kerns R, Minehart R, Ziock K, Bercaw RW, Vincent JS, Johnson R (1974). Elastic Scattering of Negative Pions from ^{16}O and Ca in the 3,3 Resonance Region. Phys. Rev. C 10:2247-2256.

Clough AS, Turner GK, Allardyce BW, Batty CJ, Baugh DJ, McDonald WJ, Riddle RAJ, Watson LA, Cage ME, Pyle GJ, Squier GTA (1974). Pion-Nucleus Total Cross Sections from 88 to 860 MeV. Nucl. Phys. Lett. B76:15-28.

Ebrahim AA, Khallaf SA (2005). Pion-^{12}C Nucleus Optical Potential. Acta Phys. Pol. B 36:2071-2085.

Eisenberg J, Koltun D (1980). Theory of Meson Interaction with Nuclei. John Wiley and Sons, New York.

El-Azab Farid M, Ebrahim AA (2015). Analysis of $\pi^{\pm}$ - nucleus elastic and inelastic scattering using the single folding α–cluster Model. Phys. Scr. 90:015301-015313.

Eriscson T, Weise W (1988). Pions and Nuclei. Clarendon Press, Oxford England.

Fäldt G (1972). On the Pion-Nucleus Interaction in the (3, 3)-Resonance Region. Phys. Rev. C 5:400-412.

Fröhlich J, Schlaile HG, Streit L, Zingl H (1981). An Improvement of Coulomb Corrections in the Phase Shift Analysis of Elastic $\pi^{\pm}-^{16}O$ Scattering and Predictions of Cross Sections for $\pi^{-}-^{16}O$ Scattering at Low Energies. Z. Phys. A – Atoms Nuclei 302:89-94.

Germond JF, Wilkin C (1977).Why Are The Diffraction Minima in π^{+} and π^{-} Scattering from ^{12}C so Different? Phys. Lett. 68B:229-233.

Gmitro M, Kamalov S, Mach R (1987). Pion-Nucleus scattering at Low and Resonance Energies. Prog. Theor. Phys. Suppl. 91:60-72.

Hirata M, Koch JH, Lenz F, Moniz EJ (1979). Isobar Hole Doorway States and pi O-16 Scattering. Ann. Phys. 120:205-248.

Hong SW, Kim BT (1999). Phenomenological local potentials for π^{-} + ^{12}C scattering from 120 to 766 MeV. J. Phys. G. Nucl. Part. Phys. 25:1065-1078.

Ingram Q, Boschitz E, Pflug L, Zichy J, Albanese JA, Arvieux J (1978). The Elastic Scattering of π^{+} and π^{-} by ^{16}O and ^{40}Ca Across the (3,3) Resonance. Phys. Lett. 76B:173-175.

Johnson MB, Satchler GR (1996). Characteristics of Local Pion-Nucleus Potentials that are Equivalent to Kisslinger-Type Potentials. Ann. Phys. (New York) 248:134-169.

Khallaf SA, Ebrahim AA (2000). Analysis of $\pi^{\pm}$ - nucleus elastic scattering using a local potential**.** Phys. Rev. C 62:024603-1-8.

Khallaf SA, Ebrahim AA (2005). Phenomenological Local Potential Analysis of π+ Scattering. FIZIKA B 14:333-348.

Kisslinger LS (1955). Scattering of Mesons by Light Nuclei. Phys. Rev. 98:761-765.

Kisslinger LS, Wang WL (1976). The Isobar-Doorway Theory for Pion-Nucleus Interactions. Ann. Phys. 99:374-434.

Koch JH, Sternheim MM (1972). Models for $\pi^{+}-^{16}O$ Scattering at 270 MeV. Phys. Rev. C 6:1118-1120.

Lee TSH, Redwine RP (2002). Pion-Nucleus Interactions. Ann. Rev. Nucl. Part. Sci. 52:23-63.

Phatak SC, Tabakin F, Landau RH (1973). Pion-Oxygen Elastic Scattering in the 3-3 Resonance Region. Phys. Rev. C 7:1803-1809.

Piffaretti J, Corfu R, Egger JP, Gretillat P, Lunke C, Schwarz E, Perrin C, Preedom BM (1977). Comparison of the π^{+} and π^{-} Elastic Scattering from ^{12}C over the πN (3,3) Resonance Region. Phys. Lett. 71B:324-326.

Rahman Md, Sen Gupta HM (1991). Strong Absorption Model for Pion–Nucleus Scattering around the (3,3) Resonance. Phys. Rev. C 44:2484-2492.

Safari R (2005). A Local Potential with Analytical Distorted Wave Approximation Model for Elastic Scattering of Pions from A Nucleus. Int. J. Pure Appl. Math. 23:283-289.

Satchler G (1992). Local potential model for pion-nucleus scattering and π^{+}/π^{-} excitation ratios. Nucl. Phys. A 540:533-576.

Shalaby AS, Hassan MYM, and Al-Gogary MM (2007). Multiple Scattering Theory for Pion-Nucleus Elastic Scattering and the In-Medium πN Amplitude. Braz. J. Phys. 37:388-397.

Shehadeh ZF (1995). PhD Thesis, Department of Physics, Southern Illinois University, Illinois, USA.

Shehadeh ZF (2008). Analysis of Low-Energy π^{+}-^{40}Ca Elastic Scattering Data. Proceedings of the 4th annual meeting of the Saudi Physical Society (SPS4), Edited by A. D. Alhaidari, H. A. Alhendi, and H. Bahlouli, Riyadh, 11-12 November, 2008 (KACST, Riyadh, 2009:24-30.

Shehadeh ZF (2009). Analysis of Pion-^{40}Ca Elastic Scattering Data using the Klein-Gordon Equation. Int. J. Mod. Phys. E 18:1615-1627.

Shehadeh ZF (2013a). Analyses of Elastically Scattered Charged Pions from ^{40}Ca in the Intermediate-Energy Region. J. Assoc. Arab Univ. Basic Appl. Sci. 14:32-37.

Shehadeh ZF (2013b). Analyses of elastically scattered charged pions from calcium isotopes and the ^{48}Ca-^{54}Fe isotone at 180 MeV. Turk. J. Phys. 37:190-197.

Shehadeh ZF (2014a). Analyses of $\pi^{\pm}$-^{12}C Elastic Scattering and Reaction Cross Section Data Below, Atop and Above the Δ – Resonance. J. Mod. Phys. 5:341-352.

Shehadeh ZF (2014b).Analyses of $\pi^{\pm}$-^{12}C Elastic Scattering Data at 100 MeV using Inverse Scattering Theory and Klein-Gordon Equation. Int. Rev. Phys. 8:110-116.

Shehadeh ZF (2014c). Analyses of Low-Energy π^{-}-^{12}C Elastic Scattering Data. J. Mod. Phys. 5:1652-1661.

Shehadeh ZF (2015a).A Full Relativistic Treatment in Analyzing α-^{12}C and α- ^{40,42,44,48} Ca Elastic Scattering Data at 1.37 GeV. Turk. J. Phys. 39:199-207.

Shehadeh ZF (2015b). Analyses of Alpha-Alpha Elastic Scattering Data in the Energy Range 53.4-119.9 MeV. Can. J. Phys. 93:1-7.

Shehadeh ZF, Al-Shawaf RM (2015). Analyses of $\pi^{+}-^{12}C$, ^{16}O Elastic Scattering Data at $T_{\pi} \leq 80\ MeV$: A Suggested Scaling Method. Mexican J. Phys. E Submitted.

Shehadeh ZF, Sabra MS, Malik FB (2003). Pion-40Ca Potential using Inverse Scattering Formalism and the Klein-Gordon Equation. Condensed Matter Theories 18:339-346.

Shehadeh ZF, Scott JS, Malik FB (2011). Analyses of $\pi^{\pm}$-^{40}Ca Elastic Scattering Data in the Delta Resonance Region using Inverse Scattering Theory and the Klein-Gordon Equation. Am. Institute Phys. J. 1370:185-191.

Stricker K (1979). PhD Thesis, Department of Physics, Michigan State University, Michigan, USA.
Stroot JP (1973). Experiments in Pion Nucleus Physics. Proceedings of LAMPF Summer School, LA-5443-C, edited by Gibbs WR, Gibson BF, July 23-26, 1973:1-13.
Walker GE (1973). Pion-Nucleus scattering assuming a separable microscopic pion-nucleon interaction. Lectures from the LAMPF Summer School on the Theory of Pion-Nucleus Scattering, LA-5443-C (July 23-26):72-86.
Zhang Y (1993). Pion-nucleus scattering and the Interacting Boson Model. Commun. Theor. Phys. 20:81-88.